Available online at www.sciencedirect.com
SCIENCE DIRECT®
Journal of the European Ceramic Society 25 (2005) 1551–1564
www.elsevier.com/locate/jeurceramsoc

Drying mechanisms and stress development in aqueous alumina tape casting

J. Kiennemann[a], T. Chartier[a,*], C. Pagnoux[a], J.F. Baumard[a], M. Huger[b], J.M. Lamérant[c]

[a] *UMR-CNRS 6638, SPCTS-ENSCI, Laboratoire Science des Procédés Céramiques et de Traitements de Surface, 47 Avenue Albert Thomas, Limoges Cedex 87065, France*
[b] *Groupe d'Étude des Matériaux Hétérogènes (GEMH), ENSCI, Limoges Cedex 87065, France*
[c] *Aluminium Pechiney, BP54, 13541 Gardanne, France*

Received 18 January 2004; received in revised form 17 May 2004; accepted 23 May 2004
Available online 1 August 2004

Abstract

Mass loss, shrinkage, Young's modulus evolution and stress development of aqueous (alumina + latex) tape cast suspensions were observed during drying. Mass loss showed a constant drying rate period, followed by a falling rate period. Concurrently a linear shrinkage rate has been observed in the thickness direction, up to a drying point after which shrinkage abruptly stops. End of constant drying rate and end of shrinkage were not necessarily concomitant and depend on the latex/alumina ratio in the tape. A Young's modulus value appears in the tape cast suspensions at the transition from liquid to solid like state. Then an increase of Young's modulus is observed corresponding to latex film formation. The stresses generated by drying in the tape exhibited a first period of increase due to capillary pressure in the pores, a small relaxation immediately followed by a second stress increase due to latex film formation, and a stress plateau at the end of latex coalescence. Alumina powder granulometry and surface tension of the liquid had a preponderant influence on the first stress maximum whereas the properties of the latex and the drying conditions dominated the second stress maximum. By increasing latex proportion up to 25 wt.% on alumina basis, it was possible to make the first and the second stress rise concomitant.

Keywords: Drying; Tape casting; Al_2O_3; Residual stresses

1. Introduction

The tape casting technique consists in depositing a thin layer of a suspension on a carrier surface, generally using the doctor blade technique.[1] After drying, a flexible green sheet is obtained with a thickness ranging from about 20 μm to more than 1 mm. Tape casting has been the most widely used technique for large-scale fabrication of thin ceramic substrates for electronic applications for many years.[2–4] Until now, the most common way to perform tape casting is to use slurries containing organic solvents taking advantage of their easy evaporation during drying step and of their good wetting properties. However, these organics require special precaution concerning flammability and toxicity. Evident environmental considerations encourage research for alternative solutions. In this respect, aqueous tape casting offers the advantages to be less environmentally hazardous and to be low cost. The development of such formulations has been the subject of recent research.[5–7] Latex binders were found to be appropriate for aqueous tape casting because they provide both low viscosity and high solid loading of the suspension that allows to reduce the amount of water to be removed during drying.

Nevertheless, aqueous tape casting of alumina is not still widely adopted by industry, because drying remains a critical step that is not perfectly controlled, mainly for large thicknesses. First the drying time is longer than in the case of

* Corresponding author. Tel.: +33 5 5545 2222; fax: +33 5 5579 0998.
E-mail address: t.chartier@ensci.fr (T. Chartier).

0955-2219/$ – see front matter © 2004 Elsevier Ltd. All rights reserved.
doi:10.1016/j.jeurceramsoc.2004.05.028

organic solvents and secondly, the probability of defect occurrence like air bubbles or a crack is much higher.

Aqueous tape casting requires, in a first stage, to define a formulation with adapted rheological behaviour. A suspension composed of alumina powder and latex emulsions is a binary colloidal suspension. To obtain a homogeneous suspension with a high solid loading (ceramic + organic particles), and then with a low amount of water to remove during drying, the stability between ceramic particles and between latex and ceramic particles should be achieved.[8]

In a second step, the drying process of the water based (alumina + latex) tapes, and the causes of cracking must be understood. Drying of green sheets is not isotropic because evaporation occurs only at the surface of the tape in contact with air. The shrinkage takes place in the thickness direction, as the green tapes stick to the support during drying. Both non-isotropic drying and shrinkage lead to stresses that develop in the tape and can initiate cracking. Martinez and Lewis[9] have recently shown that the ceramic phase dominates the initial period of stress rise, while the latex phase strongly influences residual stresses in the tape. Chiu et al.[10,11] studied the influence of slip casting processing variables on cracking of binder free alumina films using statistical methodology. They found that particle size, dispersion stability and sedimentation have an influence on crack sensitivity whereas airflow rate and surface tension have no significant influence.

In the present work, shrinkage and weight loss were simultaneously investigated in order to understand the drying kinetics of the suspensions just after casting by varying latex/powder ratio. Then, tape consolidation was studied through the measurement of the Young's modulus evolution during drying. Finally, the apparition of stresses in green sheets during drying of various suspensions and under different drying conditions was investigated in order to identify parameters that exert a preponderant influence on cracking sensitivity.

2. Experimental procedure

2.1. Suspension formulations

Three α-Al_2O_3 powders from Aluminium Pechiney (Gardanne, France) were used: ground P122 (G-P122), ground P662 (G-P662), and P172SB with respective median particle sizes of 2.8, 2.1, and 0.41 μm.

Three acrylic latex emulsions B1000, B1014 and B1007 (Rohm and Hass Co., Philadelphia, PA) with glass transition temperatures of -26, 19 and 40 °C, respectively, were used as binders in the green sheets. Acrylic particles dispersed in water are roughly spherical, with mean particle sizes of 310, 120 and 40 nm and with solid loadings of 55, 45, and 37 wt.%, for B1000, B1014 and B1007 grades, respectively.

An aqueous acrylic copolymer (CE651, Coatex, Genay, France) was used as dispersant in alumina suspensions.

A polysiloxane defoamer (BYK-035, BYK Chemie GmbH, Wesel, Germany) was used to eliminate air bubbles trapped in the suspensions. In addition, a dimethylpolysiloxane modified polyether surfactant (BYK-348, BYK Chemie GmbH) was used in some suspensions to lower the surface tension of the liquid phase.

All the suspensions were prepared using the same procedure. Alumina suspensions were prepared by planetary milling Al_2O_3 powder in deionized water, with CE651 dispersant at a concentration of 1 mg m^{-2} of powder, and with latex emulsion. As acrylic emulsions used as binder bring the major quantity of water of the tape casting suspension, all the constituents, including the binder, are introduced all together in one stage, then differs from the two stages conventional preparation of organic suspensions for tape casting. In order to verify that the latex binder was not degraded during milling, two low powder concentrated suspensions were prepared: one using the two stages conventional method and the second using the present one stage method. The rheological behaviour and the viscosity of the two suspensions, and the mechanical properties of the green sheets were identical.

The planetary milling was performed in two steps. In the first step only 70% of the total amount of alumina powder and 70% of the total amount of dispersant were introduced, in the presence of the totality of water and of latex emulsion. After 1-h milling, alumina suspension is well desagglomerated and the remaining alumina and dispersant were added, followed by a second step of 2 h ball milling. The powder was fully deagglomerated after this two stages planetary milling. 0.03 wt.% BYK-035 defoamer on the base of alumina weight and variable content of BYK-348 surfactant were added at the end of the ball milling. The obtained suspensions were then submitted to a slow rotation for at least 24 h for deairing. The amount of added water was adjusted to obtain suspensions with a viscosity of 1 Pa s for a shear rate of 10 s^{-1}, which is suitable for tape casting.

The reference formulation is 48 vol.% G-P662 alumina, 21 vol.% latex (corresponding to 12 wt.% on the basis of alumina powder) and 31 vol.% water. Latex is composed of both B1000 and B1014 emulsions in equal proportions. Based on this reference formulation, the grade of alumina powder, the latex concentration and the latex composition were varied in order to evaluate their respective influence.

2.2. Weight loss and shrinkage measurements

In order to record the weight loss and the shrinkage simultaneously as a function of time, a Sartorius BP 310S and a laser optical CCD displacement sensor (ILD 1800-2, Micro-Epsilon, Ortenburg, Germany) were used. The balance has a capacity of 310 g and a sensitivity of 0.001 g. The measuring range of the CCD sensor was $\pm$1 mm with a resolution of 0.2 μm.

A schematic representation of this system is illustrated in Fig. 1. The suspension was tape cast on a metallic support that can be heated. The tape cast sheet was 100 mm wide, 130 mm

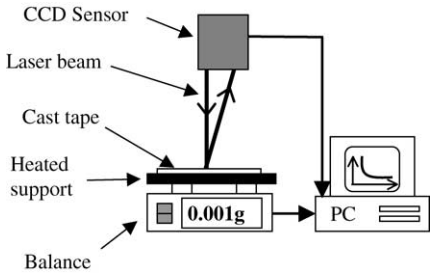

Fig. 1. Schematic representation of the weight loss and shrinkage measurements.

long, and the thickness ranged from 150 μm to more than 1 mm. After tape casting, the support was quickly placed on the balance. The mass measured with the balance decreased due to water evaporation during drying. The distance to tape cast suspension measured with the CCD sensor increased with shrinkage during drying. Then the weight loss and the shrinkage of the tape cast sheet were simultaneously recorded and monitored on a computer.

2.3. Stress measurement

Stress evolution during the drying of tape sheets was measured using a cantilever deflection technique developed by Corcoran.[12] This technique developed for determining stress in organic coatings[13–15] has been successfully used for ceramic coatings.[16,17,9] It relates the end deflection of a clamped substrate to the stress developing in a suspension deposed on the substrate during drying. A schematic of the device is illustrated in Fig. 2. Deflection was measured with a laser optical CCD displacement sensor (ILD 1800-2, Micro-Epsilon). The data were recorded on a computer. All measurements were made with the axis of the laser located at an exactly known and fixed distance from the substrate clamping point. The suspension was spread on the metallic substrate by means of a doctor blade whose translation was achieved by an electric motor. The casting velocity was fixed at 1 cm s^{-1} for a gap height of 400 μm. The suspensions can either be dried at room temperature (20 °C) or in a heated box up to 50 °C. The relative humidity of the room during drying can also be controlled.

The average in plane stress $\sigma(t)$ in the applied coating can be estimated from the measured substrate deflection by the following expression:[12]

$$\sigma(t) = \frac{dE_s e_s{}^3}{3e_c(t)L^2(e_s + e_c(t))(1-\nu_s)} + \frac{dE_c(t)(e_s + e_c(t))}{L^2(1-\nu_c(t))} \quad (1)$$

where ν_s and $\nu_c(t)$ are the substrate and the tape Poisson's ratios; E_s and $E_c(t)$ are the substrate and the tape elastic modulus; e_s and $e_c(t)$ are the substrate and the tape thickness; L is the free length of the substrate (Fig. 2). $E_c(t)$, $e_c(t)$ and $\nu_c(t)$ are quantities that vary with time t of drying. Parameter d is the end deflection of the cantilever substrate. The cantilever substrates used were stainless steel AISI 316L cut to obtain 50 mm × 6 mm clamped dimension. The properties of such substrates are: E = 200 ± 10 GPa, ν_s = 0.29, e_s = 200 μm, L = 50 mm.

The validity of the formula (1) is submitted to the following assumptions: spherical deflection of the cantilever, deformation within the elastic limits of the coating and of the substrate, isotropic mechanical properties of the coating and of the substrate, and internal stress constant through the coating thickness.

In Eq. (1), σ represents a biaxial in-plane stress averaged across the coating thickness. In many systems, as it is the case for our suspensions, the final stress is independent of the coating thickness, leading to the conclusion that in-plane stress is uniform across the thickness. The instantaneous tape thickness, $e_c(t)$, is larger than the final thickness, $e_c(t_f)$. If the final thickness is used to calculate the stress data, the stress data reported for short times of drying would be artificially high. This is the reason why, in the present work, the instantaneous coating thickness was estimated from the final coating thickness ($e_c(t_f)$) and from the shrinkage behaviour of the suspension. As the substrate is mounted horizontally in the measurement apparatus, weight loss due to evaporation also induces a deflection of the substrate. This effect of weight loss is subtracted from the measured data.

The second term of Eq. (1) expresses the stress relaxation in the tape due to the bending of the substrate. When $E \gg E_c(t)$ and/or $e_s \gg e_c(t)$, this second term can be neglected. In the present experiments, the final tape thickness varies from 100 to 250 μm, and then e_s and $e_c(t)$ are in the same range. During drying, the Young's modulus $E_c(t)$ varies from 0 (liquid) to the Young's modulus of the green tape. This parameter is quite difficult to evaluate during drying and the second term of Eq. (1) is always neglected in the literature.[13–17] Then the measurement of this term is the purpose of the next paragraph.

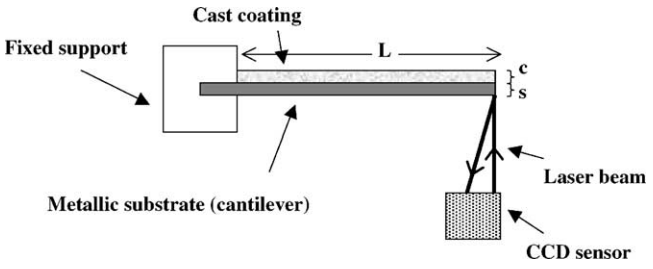

Fig. 2. Schematic representation of the cantilever deflection measurement by laser optical CCD displacement sensor.

2.4. Young's modulus measurement

Ultrasonic measurements of Young's modulus have been performed using a pulse-echo method in a "long bar mode".[18] Wide band pulses of ultrasonic compressional waves were generated by a magnetostrictive transducer and propagated through a rectangular sample via a remendur waveguide. The

suspensions were cast in a silicon mould with a 6 mm^2 rectangular section and a 100 mm length, and the waveguide was introduced in the suspension at a depth of 0.5 mm. The diameter of the remendur waveguide was 1.5 mm.

For propagation in "long bar mode", the wavelength must be larger than the cross dimensions of the propagation medium. During drying, an electronic device automatically measured and recorded the time $\tau(t)$ between echos of interest, and the reflective coefficient $R(t)$ of the acoustic wave at the interface between the guideline and the sample (Fig. 3).

From longitudinal ultrasonic velocity $V(t)$ in the "long bar mode", Young's modulus can easily be obtained by:[2]

$$E_c(t) = \rho_c(t)V(t)^2 = \rho_c(t)\left(\frac{2L_c}{\tau(t)}\right)^2 \quad (2)$$

where L_c and $\rho_c(t)$ are sample length and density, respectively. The problem in determining Young's modulus by Eq. (4) is that no echo is visible until the cast suspension became rigid. Then Young's modulus can only be accurately determined by Eq. (2) in the final period of drying.

An other less conventional way to evaluate Young's modulus during early stage of drying is to use reflective coefficient value $R(t)$. In "long bar mode", the measured value of $R(t)$ is related to the longitudinal ultrasonic velocity $V(t)$ in the sample via the acoustic impedances Z_g and Z_c of the waveguide and of the cast sample suspension by Eq. (3):

$$R(t) = \frac{Z_c - Z_g}{Z_c + Z_g} = \frac{(\rho_c(t)V(t)S(t)) - Z_g}{(\rho_c(t)V(t)S(t)) + Z_g} \quad (3)$$

where $S(t)$ is the rectangular section of the sample.

Then, Young's modulus of the sample can be obtained from the reflective coefficient $R(t)$:

$$E(t) = \frac{Z_g^2}{\rho_c(t)S(t)^2}\left(\frac{R(t)+1}{R(t)-1}\right)^2 \quad (4)$$

Eq. (4) presents the advantage, in comparison to Eq. (2), to allow the Young's modulus calculation during the whole stage of drying. It has been checked that Eqs. (2) and (4) lead to similar values of the Young's modulus in the domain for which overlap is possible from an experimental point of view.

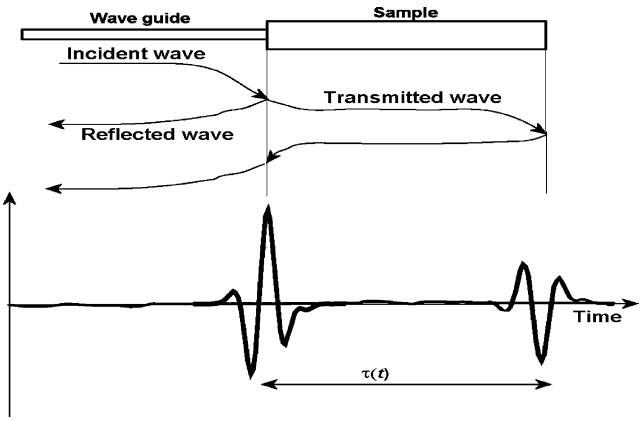

Fig. 3. Ultrasonic measurement of Young's modulus.

2.5. Surface tension measurement

The suspensions contain a solid phase (alumina + latex) and a liquid phase (water + dispersant + surfactants). The surface tension of the liquid phase has been determined by the stalagmometer method. The weight of the droplets of a liquid that flows out a fine capillary tube is proportional to the surface tension γ of the liquid and to the radius of the tube extremity. The number of droplets N that flow out for a given volume is counted. The stalagmometer is calibrated with 20 °C pure water of density ρ_0 and surface tension γ_0 = 73 mN m^{-1}. The surface tension of a liquid of density ρ is given by:

$$\gamma = \gamma_0 \frac{\rho}{\rho_0}\frac{N}{N_0} \quad (5)$$

2.6. Wetting angle measurement

The wetting angle of the liquid phase (water + latex emulsions + surfactants) was measured on an alumina substrate. A drop of a liquid was deposited on the substrate with a syringe and the observation of the drop profile was performed using a CCD camera linked to a computer. A numerical analysis of the outline of the drop leads to the value of the wetting angle.

2.7. Porosity measurement of dried green tapes

The porosity of green alumina sheets (before burnout) was measured using mercury porosimeter (AutoporeII Micromeritics 9200).

3. Results

3.1. Weight loss and shrinkage during drying

Weight loss and shrinkage are two consequences of the drying of the tape cast sheets. The drying mechanisms of systems like tape cast aqueous alumina suspension can be approached through a study of their kinetics. The weight loss and the simultaneous shrinkage of a suspension containing 12 wt.% latex, cast with a final height of 700 μm, are reported in Fig. 4. The variation of the weight loss w versus time can be fitted with two different equations depending on the drying period:

$$\text{a linear stage :} \quad w = c_r t, \quad t \le t_1 \quad (6)$$

where c_r is the first constant rate of drying.

$$\text{a falling rate stage :} \quad w = w_m - w_c\, e^{-kt}, \quad t > t_1 \quad (7)$$

where k and w_c are parameters of the fit, and w_m is the weight loss after total drying.

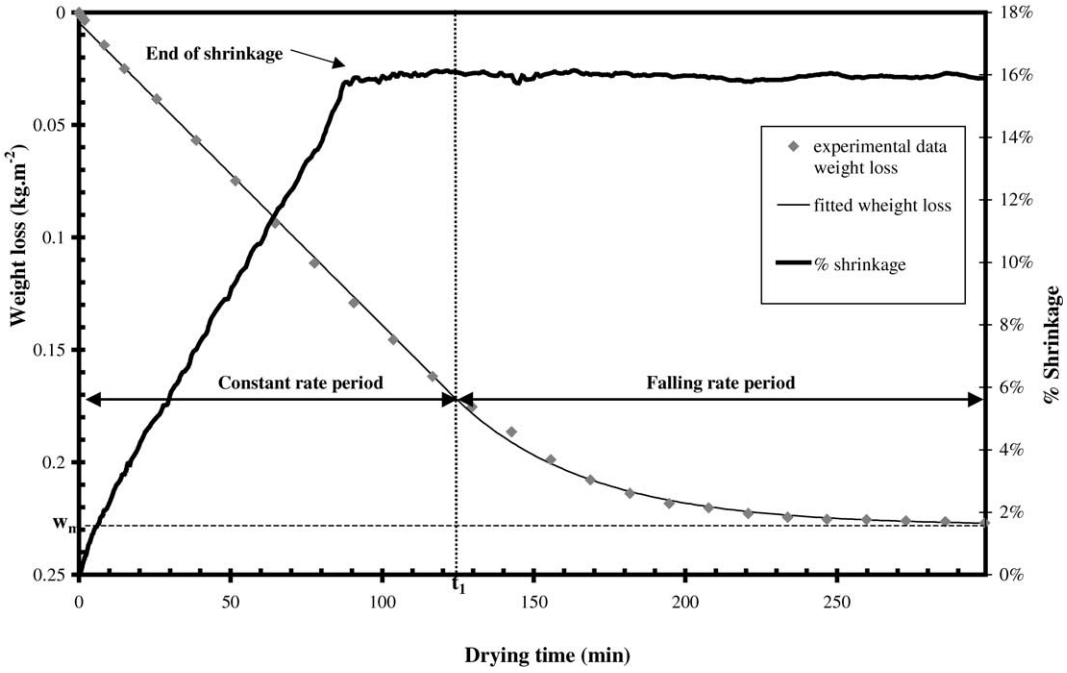

Fig. 4. Weight loss and shrinkage of a tape cast G-P662 suspension containing 12 wt.% latex with a final height of 700 μm. Relative humidity (HR) = 55%, temperature (T) = 20 °C.

The different parameters t_1, c_r, w_m, k and w_c, are calculated for the global function of weight loss versus time in order to fit at best the experimental data and to obtain a continuous function.

Just after casting, the temperature has yet to reach the wet temperature equilibrium. That's why the rate is slightly higher at the very beginning of drying than after a few minutes. When equilibrium is reached, the drying loss follows a linear stage (Eq. (6)) during which the liquid is transported to the surface of the tape by capillary forces and then evaporates (Fig. 5). In this constant rate period, the surface remains saturated with water and the drying is mainly controlled by external conditions like temperature and humidity of the drying air flow.[19–21] The transition, from the constant rate to the falling rate stage (Eq. (7)), occurs when the fluid phase does not redistribute to the top surface at a rate equivalent to the evaporation rate c_r. At this stage, the liquid phase recedes into the porous body and the drying mechanism is controlled by a diffusion process of the water to the surface through the porosity.

Concurrently to weight loss, the tape undergoes shrinkage during drying. In the first stage, the volume variation of the tape corresponds to the volume of liquid evaporated, so that the liquid/gas interface remains at the surface of the tape (Fig. 5).[22–24] The value of shrinkage during drying is governed by the balance between the capillary pressure exerted by the liquid in the pore which causes shrinkage, and the elastic modulus of the structure which resists shrinkage. When this last contribution prevails, the shrinkage stops. As seen in Fig. 4, the shrinkage is linear as a function of drying time until it stops abruptly. The end of shrinkage corresponds to the apparition of porosity in the tape because the evaporation of water is not counterbalanced by shrinkage. The porosity opened after the end of shrinkage can be evaluated by comparing the measured thickness of the tape and the predicted thickness considering that the evaporated volume corresponds to the shrinkage volume, under the assumption that shrinkage only occurs in the tape thickness direction (Fig. 6). In the present case, the end of shrinkage happens slightly before the end

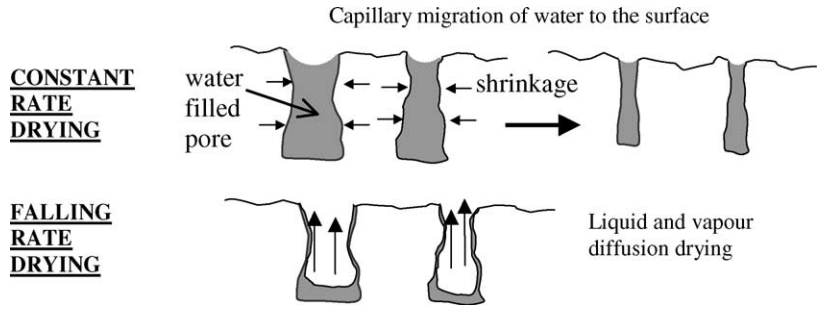

Fig. 5. Schematic representation of constant rate and falling rate drying steps in aqueous cast tapes.

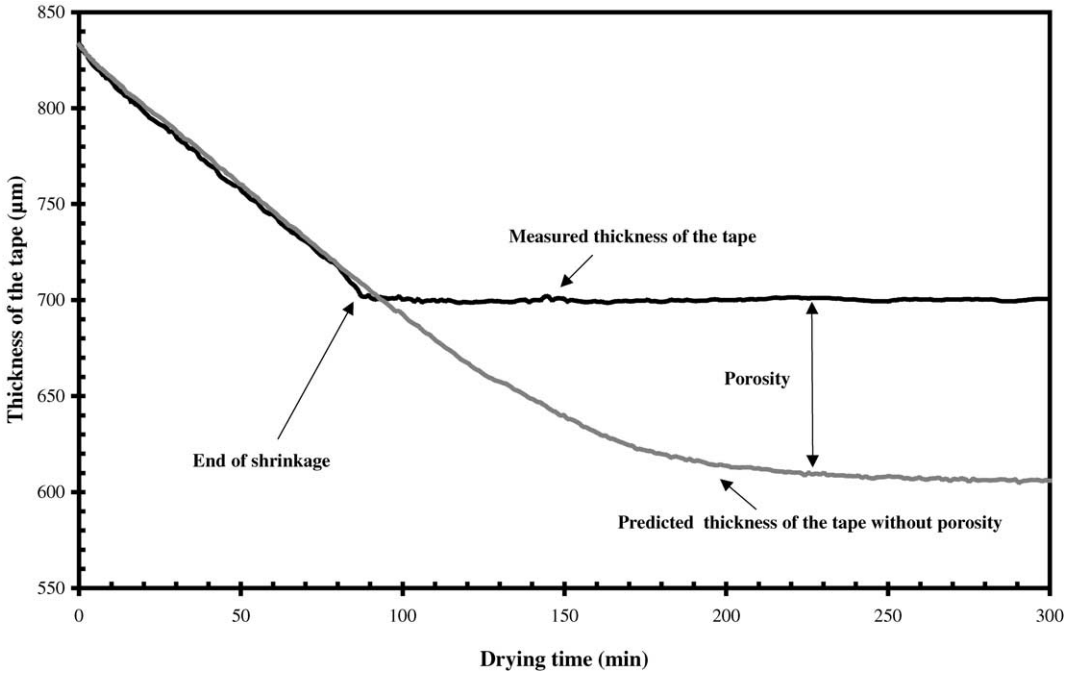

Fig. 6. Comparison, for a G-P662 suspension containing 12 wt.% latex, of the real measured thickness of the tape during drying and of the predicted thickness for a continuous shrinkage under the assumption that the evaporated volume corresponds to the shrinkage volume and that the shrinkage occurs only in the thickness direction. HR = 55%, T = 20 °C.

of the constant rate stage (Fig. 4). That means that, even if the liquid begins to recede into the pores, the drying rate is not affected for a short period. The water flow to the surface by funicular transport is still high enough compared to the evaporation rate.

In order to investigate the respective role of alumina and latex particles on the drying kinetics, different latex/alumina ratios have been tested (Table 1). The fraction of water in the tape at the end of the constant rate step increases with the amount of latex, whereas the fraction of water in the tape at the end of shrinkage decreases. When the amount of latex is low, the structure of the green tape is similar to that of a granular alumina body. Then the shrinkage stops quite quickly, because of the low mobility of alumina particles. Nevertheless, the drying rate remains constant quite a long time after the end of shrinkage. It means that water continues to reach the surface from the bulk even if a moisture gradient begins to be established in the tape thickness. For the opposite case, for large amount of latex, the shrinkage still continues after the end of the constant rate step up to reach a small fraction of remaining water in tape (i.e. 4.5 wt.%). In presence of a large amount of latex, the green tape is “soft” enough and the capillary pressure is still large enough to allow shrinkage even when the surface is no more fed by water.

3.2. Evolution of Young’s modulus during drying

The modulus of the cast tape is time dependent and rises as drying proceeds. At the beginning of drying, the cast suspension behaves as a liquid with a viscosity of 1 Pa s and the Young’s modulus is not defined. Young’s modulus of the cast suspension only appears and starts to grow when the cast sheet becomes solid like and is able to support stresses. The value of the modulus still continues to increase as long as the evaporation proceeds. Stress development in the tape results both from constrained shrinkage and from modulus rise during drying.

Table 1
Drying characteristics of green sheets cast with a G-P662 suspension containing different latex/alumina powder ratio

	Latex of alumina powder (wt.%)			
	4	12	20	50
Initial water content (%)	13.6	12.7	17.4	26.4
Drying time at critical point (min)	170	122	143	165
Water remaining in tape at the end of constant rate step (%)	2.9	4.1	5.5	8.4
Drying time at the end of shrinkage (min)	70	90	155	210
Water remaining in tape at the end of shrinkage (%)	9.0	6.4	4.6	4.5
Estimated porosity at the end of drying (%)	26.2	13.7	10.8	6.8

HR = 55%, T = 20 °C.

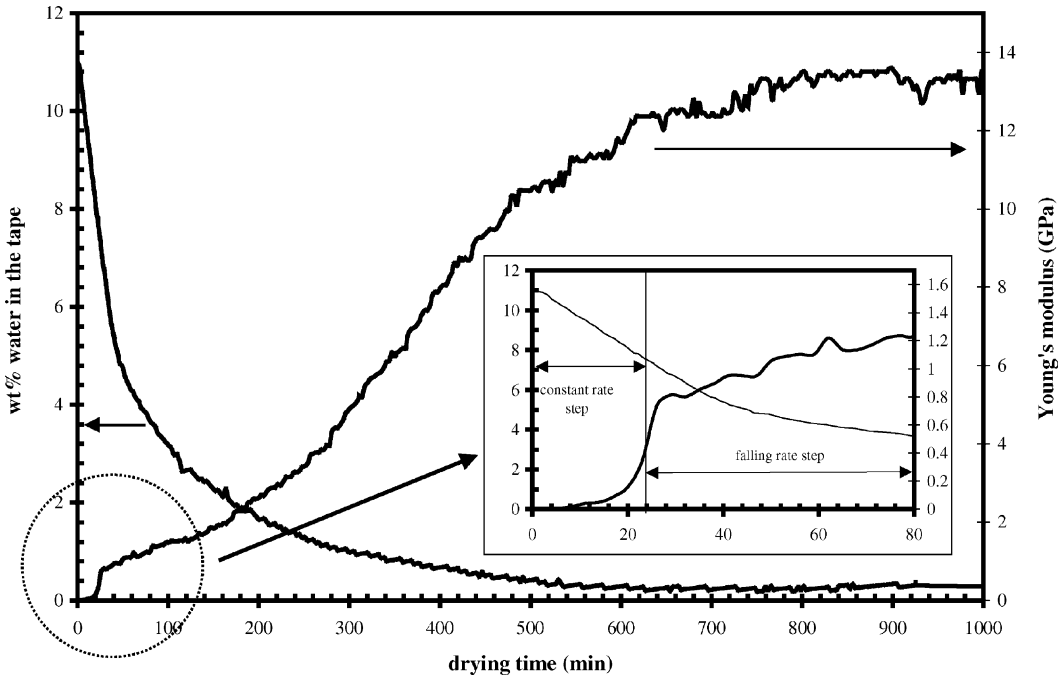

Fig. 7. Evolution of the Young's modulus and of the weight loss during drying for a G-P662 suspension containing 12 wt.% latex (2 mm thickness).

Young's modulus during drying is a very interesting parameter to determine, but not easy to measure. In order, first to evaluate the evolution of the tape rigidity during the different steps of drying and secondly to understand the stress development mechanisms in the tape, Young's modulus has been measured for two suspensions with two different latex proportions (12 and 20 wt.% on the basis of alumina powder) (Figs. 7 and 8). Because of the presence of a mould during drying and of the relatively large thickness of the body (2 mm), the drying kinetics are quite different from those observed for the thin cast tape sheets. The end of the constant rate of drying occurs for larger water concentrations in the tape, and the falling rate step/global drying time ratio is much larger than for cast tape sheets. Nevertheless, the evolution of the Young's modulus versus drying time makes it possible to observe the structural modification of the suspension

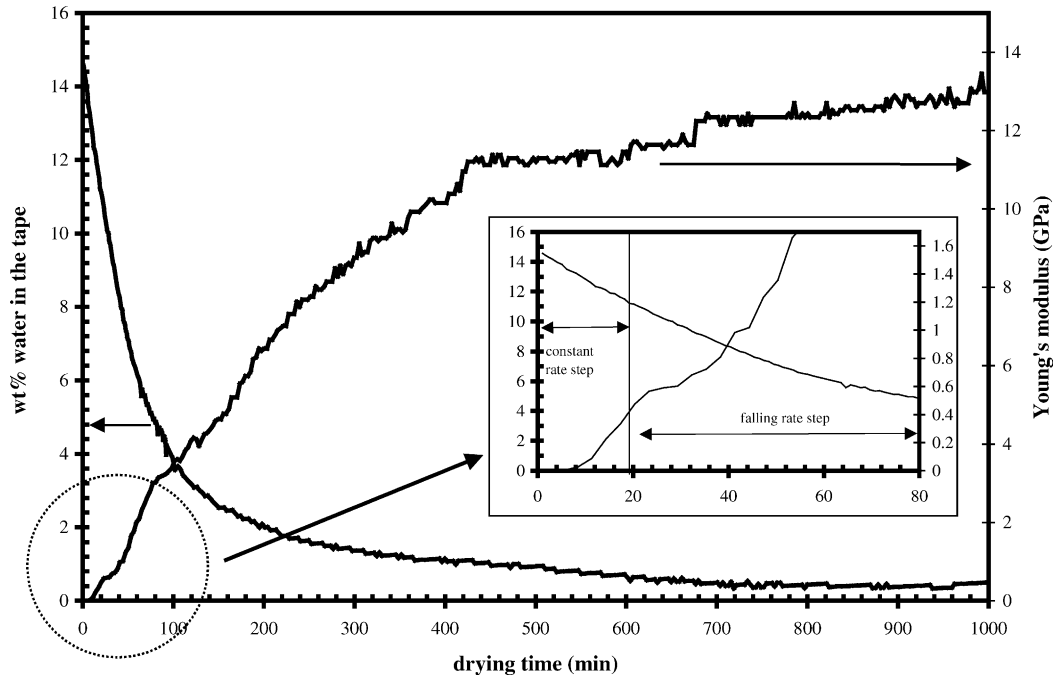

Fig. 8. Evolution of the Young's modulus and of the weight loss during drying for a G-P662 suspension containing 20 wt.% latex (2 mm thickness).

when changing from one drying step to an other. For the suspension containing 12 wt.% latex, a first abrupt increase of Young's modulus appears at the end of the constant rate period to reach about 0.8 GPa. This increase is certainly due to the transition from liquid-like to solid-like behaviour. This period is followed by a slight increase of the Young's modulus at the beginning of falling rate period. Then the Young's modulus continues to increase slowly to reach about 13 GPa at the end of drying. The structure consolidates during drying thanks to the latex film formation. For the 20 wt.% latex suspension, the evolution of Young's modulus is similar, but the first increase is less abrupt, and the slight increase at the beginning of the falling rate is more pronounced. The Young's modulus reaches, at the end of drying, the same value as that for 12 wt.% suspension, i.e. 13 GPa. The concentration of the more rigid phase, i.e. alumina, is larger in 12 wt.% latex green samples than in 20 wt.% ones but 12 wt.% latex green samples are also more porous, that could likely compensate the increase of Young's modulus.

The knowledge of the Young's modulus values of the green sheet at each drying time is of great interest to evaluate the drying stresses without neglecting the second term of Eq. (1), as is generally done in the literature due to the difficulties encountered in the measurement of this parameter.

For both Young's modulus and stress experiments, mass loss has been concurrently measured as a function of drying time. It can be assumed that, in both experiments, Young's moduli are equal for the same state of drying (amount of water still contained in the suspensions). Then, by correlating drying times between Young's modulus and stress experiments, Young's modulus can be estimated as a function of time in stress experiments.

3.3. Drying stresses

The stress behaviour evolution during drying of a representative aqueous tape cast suspension containing 12 wt.% latex is shown in Fig. 9. The cast layer exhibits a rapid period of stress rise to reach a first maximum stress (σ_{max1}), a short stress decrease period, and a second stress rise to reach a second maximum stress (σ_{max2}). Then, there is a very slow relaxation time at the end of drying. The first maximum stress approximately corresponds to the end of the constant rate step. Through neglecting the second term of Eq. (1), the first stress rise and the first stress maximum are not affected. In this case, Eq. (1) can be simplified to:

$$\sigma(t) = \frac{dE_s e_s^3}{3e_c(t)L^2(e_s + e_c(t))(1 - \nu_s)} \tag{8}$$

In contrast, the second stress rise and the second stress maximum are greatly underestimated if the second term is not taken into account. The Young's modulus of the cast tape is high enough to induce a significant contribution in Eq. (1), so that the simplified Eq. (8) is no more valid.

Stress develops during drying because of the constrained volume shrinkage associated with loss of water from the cast tape.[9] During the drying process, capillary tension developed in the liquid phase exerts a compression (P_{cap}) on the particle network, which is expressed by:[22,24]

$$P_{cap} = \frac{2\gamma \cos\theta}{r_p} \tag{9}$$

where γ is the liquid/vapor surface tension, θ is the liquid/solid contact angle, and r_p is the pore radius.

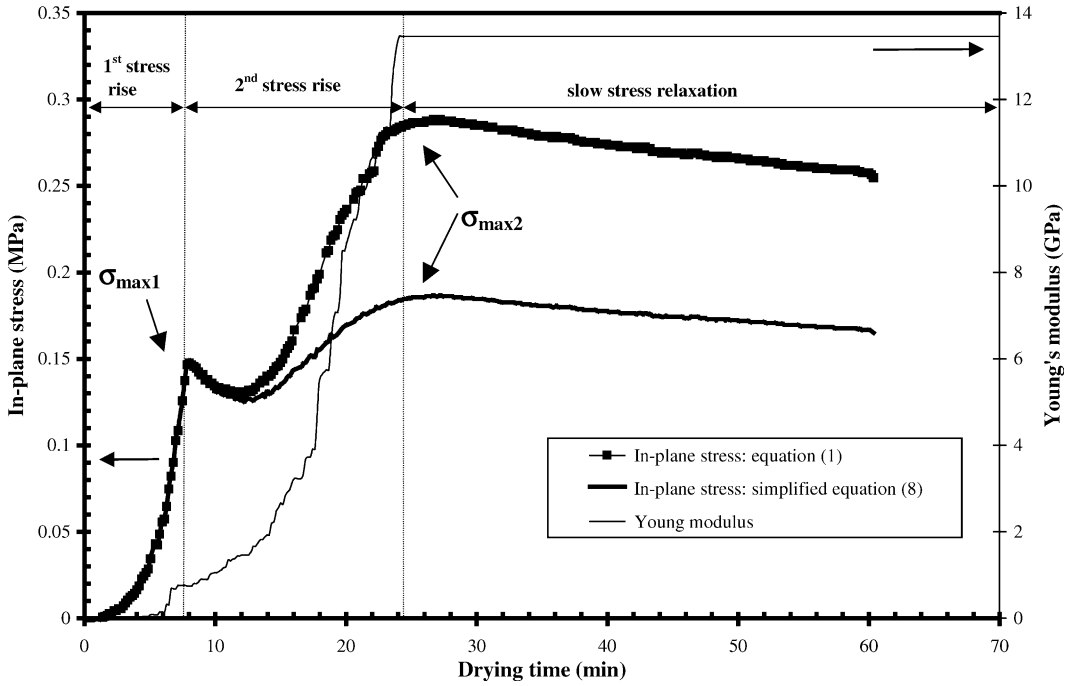

Fig. 9. Stress evolution during drying of a G-P662 suspension containing 12 wt.% latex using Eq. (1) and simplified Eq. (8). HR = 35%, T = 20 °C.

Table 2
Comparison of the calculated capillary pressure with the in-plane stress measured at the first stress peak, for different granulometries of the alumina powder (12 wt.% latex suspension)

	Powder		
	P172SB	70 wt.% G-P122; 30 wt.% P172SB	G-P122
d_{50} powder (μm)	0.41	Bimodal granulometry	2.8
d_{50} pore (μm) in the dried tape	0.13	0.28	1.0
P_{cap} (MPa) (Eq. (9))	0.88	0.41	0.115
σ_{max1} measured (MPa)	0.60	0.38	0.090

HR = 55%, T = 20 °C.

In order to reduce crack sensitivity of the tape, a solution is to reduce capillary pressure since it can be at the origin of stress increase in the tape. Two parameters can be modified to reduce capillary pressure, e.g. the median pore size, or the surface tension of the liquid phase in the suspension.

First the median pore size has been studied through the use of starting powders with different granulometries. During the first step of drying, the evaporation process leads to shrinkage and corresponding decrease in median pore size within the tape. In order to estimate the median pore size, the pore size distribution has been measured at the end of drying process. We can assume that this pore size distribution corresponds to that at the first stress maximum (σ_{max1}) since no more important shrinkage appears beyond this step. The median pore size in the tape logically decreases with the median grain size (Table 2). To reduce the pore size, a mixing of coarse and fine powders with a size ratio of 10 has also been used.[25] The $\gamma \cos\theta$ term for the liquid of those suspensions containing 12 wt.% latex has been measured and is equal to 28.8 mN m^{-1}. Then, using the median pore size for r_p, P_{cap} has been calculated, and compared to the first stress maximum value (σ_{max1}) measured in Fig. 10. P_{cap} and σ_{max1} are in reasonable agreement (Table 2). This suggests that the first maximum stress peak in the green tape at the end of the first stage of drying can be attributed to capillary forces. Then it is directly related to the pore size in the tape and to the granulometry of the starting alumina powder. Nevertheless, the powder size should be kept small enough to maintain sintering reactivity.

The second method to attenuate capillary pressure consists in reducing the $\gamma \cos\theta$ term. Accordingly, the influence of the surface tension of the liquid in the suspension on the stress generated during drying has been studied through the addition of a tensioactive agent (BYK-348, BYK Chemie GmbH) into the G-P662 suspension containing 12 wt.% latex. The pore radius in the dried tapes has been found to remain nearly constant and equal to 0.23 μm whatever the surface tension values. The surface tension and the wetting angle of each liquid have been measured to calculate the capillary pressure (P_{cap}) for comparison with the measured first stress maximum

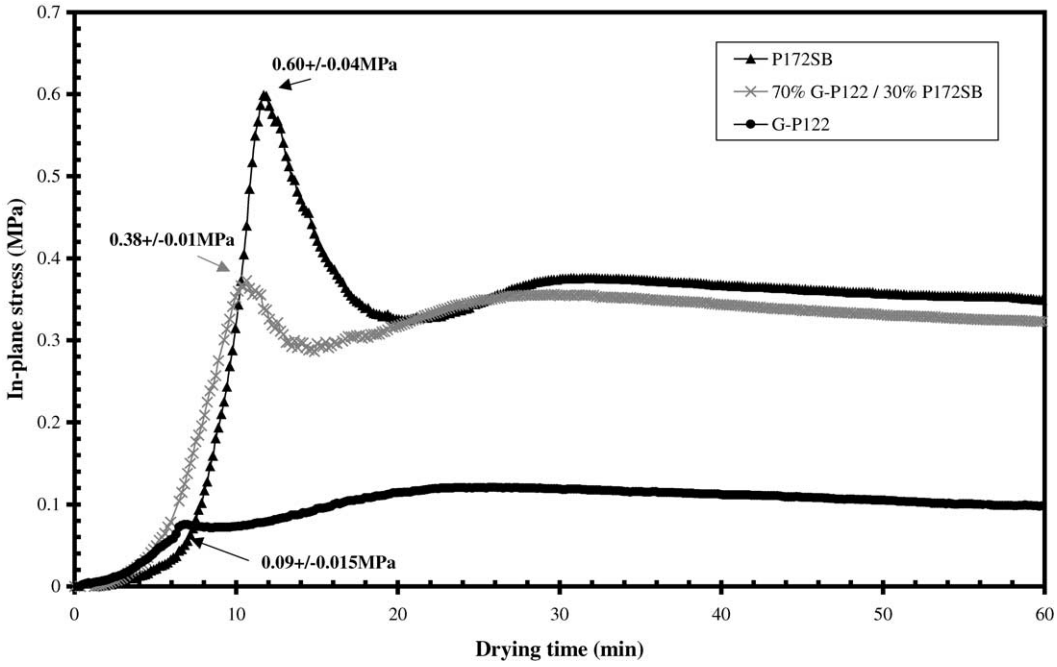

Fig. 10. Stress evolution during drying for suspensions containing 12 wt.% latex prepared with powders of different granulometries; d_{50} = 0.41 μm for P172SB, d_{50} = 2.8 μm for G-P122 and a mixture of the two powders. HR = 55%, T = 20 °C.

Table 3
Comparison of the capillary pressure with the in-plane stress measured at the first stress peak, for different weight percentage of tensioactive agent in the suspension (G-P662 suspension containing 12 wt.% latex)

	Tensioactive BYK-348 (wt.%)				
	0	0.05	0.15	0.50	1.0
γ (mN m^{-1})	48	41	33	25	21
$\cos\theta$	0.60	0.61	0.69	0.87	0.93
P_{cap} (MPa) (Eq. (9))	0.233	0.202	0.183	0.179	0.155
σ_{max1} measured (MPa)	0.157	0.127	0.112	0.092	0.092

HR = 35%, T = 20 °C.

values (σ_{max1}) (Table 3 and Fig. 11). The decrease of the σ_{max1} value with the addition of tensioactive fairly matches with the P_{cap} decrease. It is then possible to decrease the first maximum stress peak in tape cast drying and to minimize the risk of cracking by reducing the $\gamma\cos\theta$ value of the liquid in the suspension, for instance by the addition of a tensioactive agent.

It is clear that capillary pressure is the cause of the first stress rise during drying, but capillary pressure cannot explain the second part of the in-plane stress leading to a second stress maximum. Martinez and Lewis[9] showed that, for pure alumina suspensions without latex, the first stress rise is followed by a stress decay to a nearly stress-free state and no second stress rise has been observed. Then, in the present suspensions containing a latex binder, the latex is likely to be responsible for the second stress rise. To check this point, in-plane stresses have been estimated for different latex concentrations in G-P662 alumina suspensions and for a pure latex suspension (Fig. 12). The stress variations actually vary according to the latex content. Up to 18 wt.% latex, the stress variations are similar with a first stress rise, a stress relaxation and a second increase of stress. For the suspension containing 18 wt.% latex, the first stress maximum reaches a value of 0.37 MPa in comparison to 0.15 MPa for a 12 wt.% latex content, and the pore size in the dried tape is reduced down to 0.17 μm, in comparison to 0.23 μm for a 12 wt.% latex content. Nevertheless, the contribution of the pore size to capillary pressure is not high enough to explain such a stress maximum gap between 12 and 18 wt.% latex. For a latex addition larger than 18 wt.%, the stress evolution with drying time drastically changes with only one stress rise and no stress relaxation. For an addition of 25 wt.% latex, the first stress peak seems to be truncated and the maximum stress reached is much lower than for 18 wt.% latex, but the final stress values at the end of drying are similar. For latex amounts larger than 50 wt.%, the stress slowly increases up to reach a plateau during evaporation of water without stress relaxation. The maximum stress value is constant for 50 and 80 wt.% latex.

As latex is at the origin of the stress generated in the second drying part, modifying latex properties could be an interesting way to reduce stress and then crack sensitivity. Glass

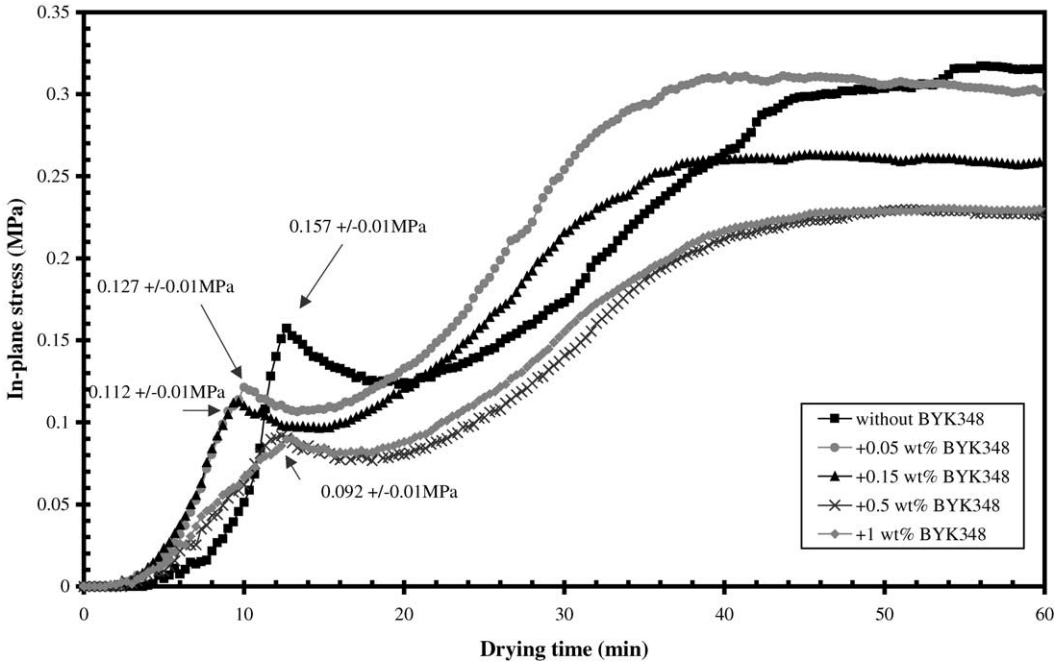

Fig. 11. Stress evolution during drying for different surface tensions and wetting angles of the liquid in the G-P662 suspension containing 12 wt.% latex (Table 3). HR = 35%, T = 20 °C.

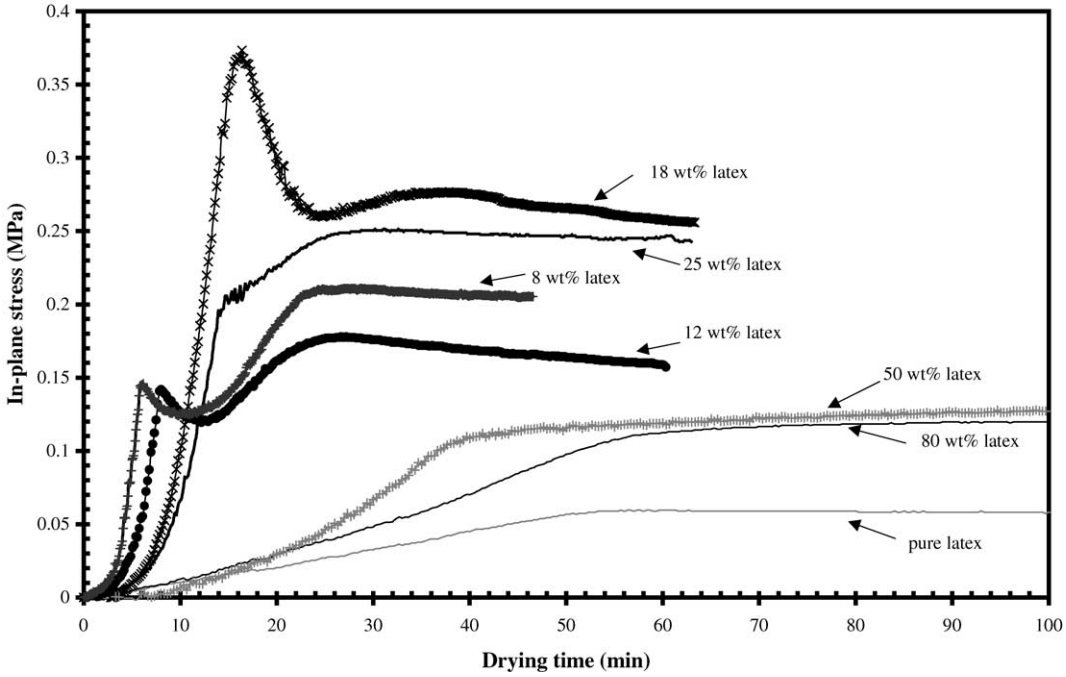

Fig. 12. Stress evolution during drying for different latex concentrations in G-P662 suspensions. HR = 55%, T = 20 °C.

temperature transition of the latex is certainly the parameter that can most influence stress generated in the tape during latex coalescence. The variations of in-plane stresses during drying of G-P662 suspensions containing 8 wt.% latex with different glass transition temperature (T_g) are shown in Fig. 13. When using a latex with a T_g (40 °C) much higher than room temperature, the tape becomes very rigid during drying, and in-plane stresses strongly increase until the decohesion between the tape and the steel substrate occurs. Latex with a high T_g is not adapted for tape casting of alumina. For latex with a T_g in the vicinity of room temperature (19 °C), or below (−26 °C), the first maximum stresses (σ_{max1}) are similar, but the second stress maximum (σ_{max2}) is lower for the low T_g latex (−26 °C). That is in agreement with the

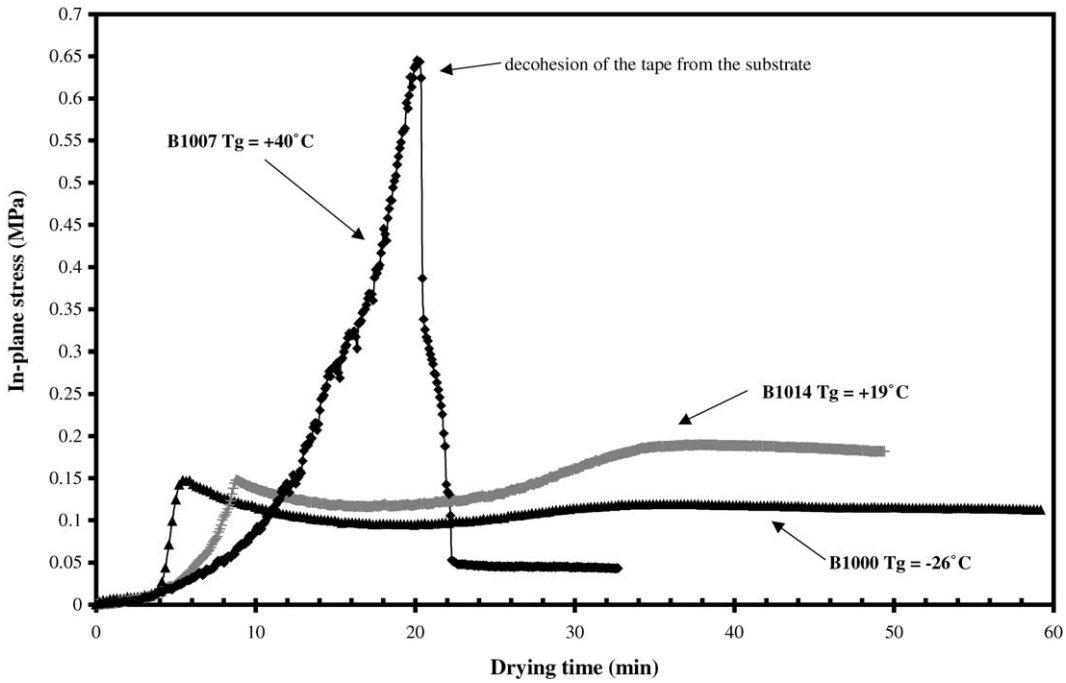

Fig. 13. Stress evolution during drying of G-P662 suspensions containing 8 wt.% latex with different glass transition temperatures. HR = 55%, T = 20 °C.

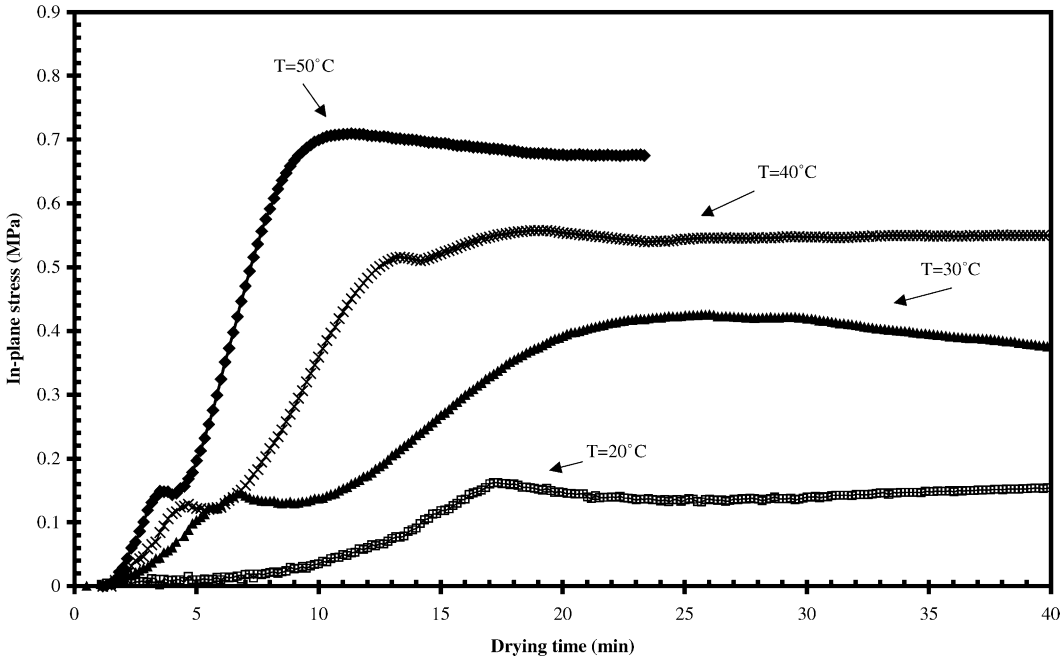

Fig. 14. Stress evolution during drying of G-P662 suspension containing 12 wt.% latex, for different drying temperatures. HR = 55%.

fact that the first stress rise is governed by capillary pressure and that the second part of in-plane stress is governed by the latex rigidification during drying. Then, only the second maximum stress value can be controlled by the nature of the latex binder.

After studying the influence of the material parameters on the stress generated in the tape during drying, extrinsic parameters like external drying conditions have been studied in order to optimize drying conditions to get low stress. Drying conditions (temperature and relative humidity) have no significant effect on the first stress rise amplitude (σ_{max1}), but they greatly influence the second stress rise (Figs. 14 and 15). When the temperature increases, and when the relative humidity of the drying air is lowered, the second stress maximum (σ_{max2}) increases. The drier the tape at the end of drying, the higher is the final stress.

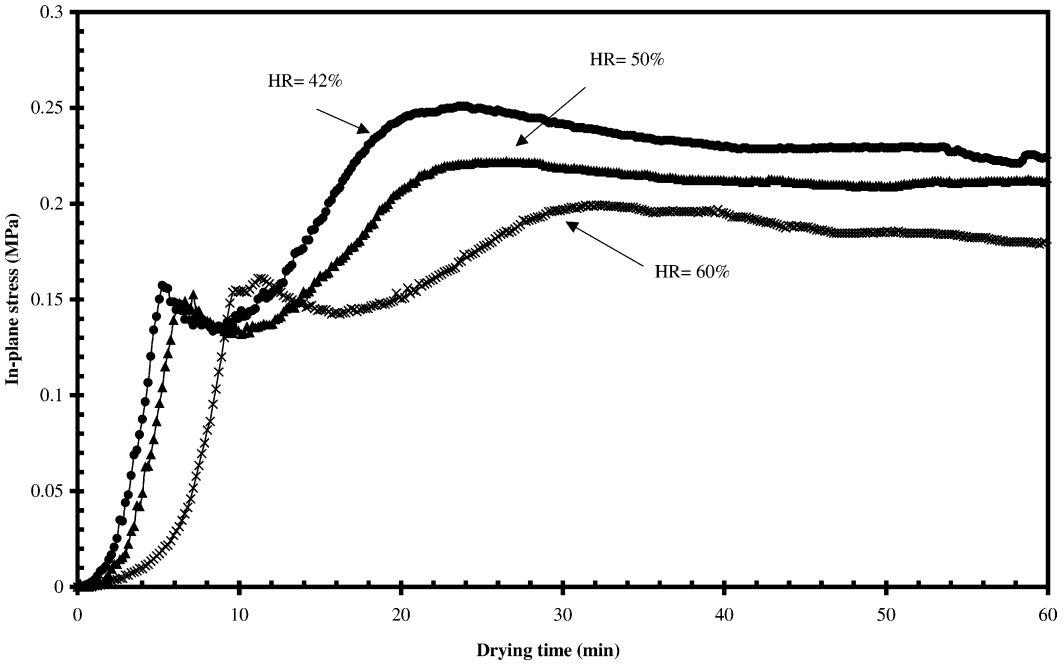

Fig. 15. Stress evolution during drying of G-P662 suspension containing 12 wt.% latex, for different values of relative humidity of drying air at 20 °C.

4. Discussion

4.1. Origin of stress in (alumina + latex) tapes

In plane stresses can develop in two ways in the tape: first, because of the capillary pressure in the pore, and secondly because of a non-isotropic drying with a moisture gradient across the thickness of the tape leading to a differential shrinkage between the top and the bottom.[10] For G-P662 (d_{50} = 2.0 μm) suspensions containing up to 12 wt.% latex, the maximum stress peak is reached when the drying rate begins to fall. For these suspensions, at the end of the constant rate step, in-plane stresses can only be attributed to capillary pressure with a stress maximum that corresponds to the capillary pressure maximum. For G-P662 suspensions containing a larger amount of latex, i.e. 18 wt.%, the maximum stress is larger than expected from capillary pressure and the first stress maximum is obtained after the end of the constant rate drying stage (Fig. 12). It means that the latex coalescence starts before the first stress maximum is reached, and that it can contribute to an additional stress. Beyond 25 wt.% of latex, the stress due to the coalescence of latex particles becomes greater than the stress due to capillary pressure. That explains why the first stress maximum is truncated and is replaced by a slow and continuous increase of stress.

Nevertheless, if the presence of latex does not affect the in-plane stress before latex coalescence, the second peak of stress (σ_{max2}) can be attributed to the latex film formation. Latex coalescence appears when the volume fraction of latex particles in the liquid phase approaches 60%.[17] That means that for higher latex content in the suspension, coalescence can occur for a higher amount of remaining water in the green tape. Latex coalescence is driven by evaporation that induces particle consolidation and deformation of the particles due to capillary pressure exerted during the second stage of drying and to polymer interfacial tension.[26] The structure of the green tape is rigidified by the coalescence of latex and leads to the second stress rise. The value of the second stress maximum (σ_{max2}) depends on intrinsic properties of latex like glass transition temperature and on its final state, which is influenced by the drying conditions. The deformation of latex particles during coalescence can depend on the system temperature and the evaporation rate.[27] It can explain why σ_{max2} increases with drying temperature and when relative humidity of the drying air is reduced.

4.2. Cracking sensitivity in (alumina + latex) tapes

The sensitivity to cracking will obviously increase with the in-plane stress. Green tape can be considered as a brittle material in a first approximation. Fracture occurs in the green tape when the stress intensity factor K, at the tip of a critical flaw of length c, reaches a critical value K_c:[28]

$$K_c = \sigma\sqrt{\pi c} \tag{10}$$

where K_c is the fracture toughness.

Then, a first source of cracks in the tape is the presence of critical defects which can initiate cracking during the drying phase.[29] To minimize the risk of cracking, suspensions should be free of defects such as agglomerates and air bubbles. The preparation of a homogeneous, well desagglomerated and stable aqueous suspension is critical.

The second source of cracks in the green tape is in plane stress generated during drying. Hu et al.[30] analyzed the mechanisms of cracking for a thin film of alumina without binder deposited on a rigid substrate. Their theory shows that there is a critical thickness above, which a tape with a given in-plane stress will spontaneously crack during drying. Then, the cracking sensitivity can be evaluated by this critical cracking thickness (CCT). The CCT is linked to the in-plane stress (σ) and to the toughness (K_c):

$$\mathrm{CCT} = \left(\frac{K_c}{1.4\sigma}\right)^2 \tag{11}$$

Even if the second stress maximum (σ_{max2}) is larger than the first stress maximum (σ_{max1}) depending on the drying conditions and on latex properties, cracking always occurs approximately at the end of the constant rate step which corresponds to the first stress rise. Initiation of cracking has never be observed at a drying time corresponding to the σ_{max2} rise, even if $\sigma_{max2} > \sigma_{max1}$. The fracture toughness and the Young's modulus of the green tape increase during drying and are much higher during the second stress rise, which corresponds to latex film formation, than during the first stress rise that corresponds to volume change of the tape.

The second stress rise is then much less crucial than the first one in terms of cracking sensitivity of the green tape. In this respect, parameters like latex glass transition temperature, temperature and humidity of drying air, are less important than parameters that directly act on the first stress rise. Then, to reduce the sensitivity to cracking and to increase the CCT value, the pore size of the green tape should be increased by increasing the particle size of the powder as far as possible in terms of sintering reactivity, and the surface tension of the liquid should be lowered.

An interesting solution to reduce cracking sensitivity is to truncate the first stress rise through its shift during the latex coalescence, then the capillary pressure maximum occurs during the latex film formation. First and second stress rises will overlap, and the mechanical properties of the green tape will become high enough at maximum stress to sustain drying stresses generated by capillary pressure. In the present system, to overlap the first stress rise and the second stress rise, the solution is to increase the concentration of latex to above 25 wt.% in the suspension (Fig. 12). Nevertheless, this solution presents the drawback to lead to a low powder packing with a relative green density of 49% for 25 wt.% latex.

5. Conclusion

Cracking occurs in the green tape when the stresses developed in the tape during drying become too large compared to the tape cohesion. Both mechanical properties and stresses in the tape change with drying time.

The consolidation of the green tape during drying has been followed by the Young's modulus evolution. A first abrupt increase of the Young's modulus at the end of the constant rate step corresponds to the transition from liquid-like to solid-like state. Then, a second Young's modulus increase during the falling rate period corresponds to the structure consolidation by latex film formation.

The in-plane stress in the tape exhibits four distinct regions in function of drying time: an initial period of stress increase due to capillary pressure in liquid pore roughly corresponding to the first constant rate drying stage, a small relaxation at the end of shrinkage, a second stress increase due to latex film formation, and a plateau or an eventual relaxation at the end of latex coalescence.

Two different ways have been found to reduce crack sensitivity. First, as cracking is much more sensitive to the first than to the second stress rise for which the tape has already begun to consolidate with enhanced mechanical properties, the first stress maximum should be lowered. Then, the evaporating rate depending on humidity and temperature of drying air, and latex properties (T_g) are not suitable parameters to prevent cracking because they only act on the second stress rise. In contrast, increasing pore size and lowering surface tension are efficient to lower capillarity pressure and first stress maximum and then, to avoid cracking of a non-fully consolidated green tape.

A second way to reduce cracking sensitivity is to make the first stress rise occur when the green tape has already begun to consolidate. That is possible by increasing latex proportion in the tape over 25 wt.% on alumina basis. Then, capillary pressure maximum occurs during the latex film formation and the mechanical properties of the green tape are large enough to sustain drying stresses.

References

1. Mistler, R. E., Tape casting: the basic process for meeting the needs of the electronic industry. *Am. Ceram. Soc. Bull.*, 1990, **69**(6), 1022–1026.
2. Fiori, C. and De Portu, G., A technique for preparing and studying new materials. *Br. Ceram. Proc.*, 1986, **38**, 223–225.
3. Chartier, T., Tape-casting. In *Encyclopedia of Advanced Materials*, ed. D. Bloor, R. J. Brook, M. C. Fleming and S. Mahajan. Pergamon Press , 1994, pp. 2763–2767.
4. Hyatt, T. P., Electronics: tape casting, roll compaction. *Am. Ceram. Soc. Bull.*, 1995, **74**(10), 56–59.
5. Kristofferson, A. and Carlstrom, E., Tape casting of alumina in water with an acrylic latex binder. *J. Eur. Ceram. Soc.*, 1997, **17**, 289–297.
6. Kristofferson, A., Roncari, E. and Galassi, C., Comparison of different binders for water-based tape casting of alumina. *J. Eur. Ceram. Soc.*, 1998, **18**, 2123–2131.
7. Doreau, F., Tari, G., Pagnoux, C., Chartier, T. and Ferreira, J. M. F., Processing of aqueous tape casting of alumina with acrylic emulsion binders. *J. Eur. Ceram. Soc.*, 1998, **18**, 311–321.
8. Ushifusa, N. and Cima, M., Aqueous processing of mullite containing green sheets. *J. Am. Ceram. Soc.*, 1991, **74**(10), 2243–2247.
9. Martinez, C. J. and Lewis, J. A., Rheological, structural, and stress evolution of aqueous Al_2O_3: latex tape-cast layers. *J. Am. Ceram. Soc.*, 2002, **85**(10), 2409–2416.
10. Chiu, R. C., Garino, R. J. and Cima, M. J., Drying of granular ceramics films: I. Effect of processing variables on cracking behaviour. *J. Am. Ceram. Soc.*, 1993, **76**(9), 2257–2264.
11. Chiu, R. C. and Cima, M. J., Drying of granular ceramics films: II. Drying stress and saturation uniformity. *J. Am. Ceram. Soc.*, 1993, **76**(11), 2769–2777.
12. Corcoran, E. M., Determining stresses in organic coatings using plate beam deflection. *J. Paint. Technol.*, 1969, **41**(538), 635–640.
13. Perera, D. Y. and Eynde, D. V., Considerations on a cantilever (beam) method for measuring the internal stress in organics coatings. *J. Coat. Technol.*, 1981, **53**(677), 39–44.
14. Townsend, P. H., Barnett, D. M. and Brunner, T. A., Elastic relationships in layered composite media with approximation of the case of thin film on a thick substrate. *J. Appl. Phys.*, 1987, **62**(11), 4438–4444.
15. Payne, J. A., McCorminck, A. V. and Francis, L. F., In situ stress measurements apparatus for liquid applied coatings. *Rev. Sci. Instrum.*, 1997, **68**(121), 4564–4568.
16. Lewis, J. A., Blackman, K. A. and Ogden, A. L., Rheological property and stress development during drying of tape-cast ceramic layers. *J. Am. Ceram. Soc.*, 1996, **79**(12), 3225–3234.
17. Smay, J. E. and Lewis, J. A., Structural and property evolution of aqueous-based lead zirconate tape-cast layers. *J. Am. Ceram. Soc.*, 2001, **84**(11), 2495–2500.
18. Huger, M., Fargeot, D. and Gault, C., High temperature measurement of ultrasonic wave velocity in refractory materials. *High Temperatures High Pressures*, 2002, **34**, 193–201.
19. Lewis, J. A., Colloidal processing of ceramics. *J. Am. Ceram. Soc.*, 2000, **83**(10), 2341–2359.
20. Briscoe, B. J., Biundo, G. L. and Ozkan, N., Drying kinetics of water-based ceramic suspensions for tape casting. *Ceram. Int.*, 1998, **24**, 347–357.
21. Sherwood, T. K., The drying of solid I. *Ind. Eng. Chem.*, 1929, **21**(1), 12–16.
22. Scherer, G. W., Theory of drying. *J. Am. Ceram. Soc.*, 1990, **73**(1), 3–14.
23. Nadeau, J. P. and Puiggali, J. R., Séchage: des processus physiques aux procédés industriels. *Technique et Documentation Lavoisier*, 1995.
24. Smith, D. M., Scherer, G. W. and Anderson, J. M., Shrinkage during drying of silica gel. *J. Non-Cryst. Solids*, 1995, **188**, 191–205.
25. Yu, A. B., Standish, N. and Mc Lean, A., Porosity calculation of binary mixtures of non spherical particles. *J. Am. Ceram. Soc.*, 1993, **76**(11), 2813–2816.
26. Eckersley, S. T. and Rudin, A., Mechanism of film formation from polymer latexes. *J. Coat. Technol.*, 1990, **780**, 89–100.
27. Keddie, J. L., Film formation of latex. *Mat. Sci. Eng.*, 1997, **21**, 101–170.
28. Griffith, A. A., The phenomenon of rupture and flows in solids. *Phil. Trans. R. Soc. Lond. Ser. A*, 1920, **221**, 1663–1693.
29. Descamps, M., Mascart, M., Thierry, B. and Leger, D., How to control cracking of tape cast sheets. *Am. Ceram. Soc. Bull.*, 1995, **74**(3), 89–92.
30. Hu, M. S., Thoules, M. D. and Evans, A. G., Decohesion of thin film from brittle substrates. *Acta Met.*, 1988, **36**(5), 1301–1307.